

Incorporation of a New Type of Transition Metal Complex into the Thioarsenate Anion: Syntheses, Structures, and Properties of Two Novel Compounds $[\text{Mn}_3(2,2'\text{-bipy})_3(\text{As}^{\text{V}}\text{S}_4)_2]_n \cdot n\text{H}_2\text{O}$ and $\text{Mn}_2(2,2'\text{-bipy})\text{As}_2^{\text{III}}\text{S}_5$

Ming-Lai Fu,^{†‡} Guo-Cong Guo,^{*†} Xi Liu,[†] Wen-Tong Chen,[†] Bing Liu,[†] and Jin-Shun Huang[†]

State Key Laboratory of Structural Chemistry, Fujian Institute of Research on the Structure of Matter, Chinese Academy of Sciences, Fuzhou, Fujian 350002, P. R. China, and Graduate School of Chinese Academy of Sciences, Beijing 100039, P. R. China

Received January 5, 2006

The incorporation of $[\text{Mn}(2,2'\text{-bipy})_2]^{2+}$ with thioarsenate resulted in the formation of two novel compounds, $[\text{Mn}_3(2,2'\text{-bipy})_3(\text{As}^{\text{V}}\text{S}_4)_2]_n \cdot n\text{H}_2\text{O}$ (**1**) and $\text{Mn}_2(2,2'\text{-bipy})\text{As}_2^{\text{III}}\text{S}_5$ (**2**), in which the main-group chalcogenide framework is incorporated with a $[\text{tm}(2,2'\text{-bipy})_m]^{n+}$ complex. Meanwhile, the tetrathioarsenate(V) anion acts as a new $\mu_3\text{-}1\kappa\text{S}:1,2\kappa\text{S}':2,3\kappa\text{S}'':3\kappa\text{S}'''$ ligand in **1**, in which all four S atoms of the $[\text{As}^{\text{V}}\text{S}_4]^{3-}$ anion are coordinating to metal. As a result, the two compounds exhibit semiconducting properties ($E_g = 2.18$ eV (**1**) and 1.83 eV (**2**)) and strong blue photoluminescence, with the emission maximum occurring at about 440 nm. Magnetic measurements show that both compounds have AF ordered states with Néel temperatures of 19 and 24 K for **1** and **2**, respectively.

Introduction

Ever-increasing interests have been paid to the incorporation of transition metals (tm's) into the main-group chalcogenide framework because of their exciting structural architectures¹ and potential application as semiconductors,² storage materials,³ and magnetic materials,⁴ etc. Whereas, in contrast with crystalline oxide-based materials, the preparation and characterization of non-oxide compounds present more experimental challenges. Furthermore, the coordination chemistry of main-group chalcogenides incorporated with tm's is still in its infant stages.⁵ A great diversity of structures and interesting properties can be expected if a tm complex is introduced into the main-group chalcogenide network. Recently, the introduction of mild hydro(solvo)-thermal techniques and the use of organic structure-directing

agents, such as en (ethylenamine) and dien (diethylenamine), etc.,⁶ has been shown to be a promising synthetic technique for the preparation of tm chalcogenides. Because of the formation preference of isolated $[\text{tm}(\text{amine})_m]^{n+}$ complexes for tm ions in the presence of strongly chelating amines, there are only a few main-group chalcogenide compounds in which tm amine complexes are incorporated into the main-group chalcogenide anionic network.⁷ Substantial success has recently been achieved with thioantimonates by using a tetradentate amine, such as tris(2-aminoethyl)amine (tren) and triethylenetetramine (trien), which coordinates to the tm ion with two free coordination sites of the tm atom in favor of further bonding with the S atoms to form the main-group chalcogenide network.⁸ Similarly, the investigation on chalcogenoarsenates is limited despite the various known tm chalcogenoarsenate(III,V) compounds.⁹ We are interested in introducing tm amine complexes into the chalcogenoarsenate framework and

* To whom correspondence should be addressed. E-mail: gcguo@ms.fjirsm.ac.cn.

[†] Fujian Institute of Research on the Structure of Matter, Chinese Academy of Sciences.

[‡] Graduate School of the Chinese Academy of Sciences.

- (1) Drake, G. W.; Kolis, J. W. *Coord. Chem. Rev.* **1994**, *137*, 131.
- (2) (a) Chen, Z.; Wang, R.; Li, J. *Chem. Mater.* **2000**, *12*, 762. (b) Powell, A. V.; Boissière, S.; Chippindale, A. M. *J. Chem. Soc., Dalton Trans.* **2000**, 4192.
- (3) Zheng, N.; Bu, X.; Wang, B.; Feng, P. *Science* **2002**, *298*, 2366.
- (4) Stephan, H.-O.; Kanatzidis, M. G. *J. Am. Chem. Soc.* **1996**, *118*, 12226.
- (5) Cheetham, A. K.; Férey, G.; Loiseau, T. *Angew. Chem., Int. Ed.* **1999**, *38*, 3269.

- (6) (a) Sheldrick, W. S.; Wachhold, M. *Coord. Chem. Rev.* **1998**, *176*, 211. (b) Sheldrick, W. S. *J. Chem. Soc., Dalton Trans.* **2000**, 3041. (c) Li, J.; Chen, Z.; Wang, R.; Proserpio, D. M. *Coord. Chem. Rev.* **1999**, *190–192*, 707.
- (7) (a) Bensch, W.; Schur, M. *Eur. J. Solid State Inorg. Chem.* **1996**, *33*, 1149. (b) Schur, M.; Näther C.; Bensch, W. *Z. Naturforsch., B: Chem. Sci.* **2001**, *56*, 79. (c) Bensch, W.; Näther, C.; Schur, M. *Chem. Commun.* **1997**, 1773. (d) Fu, M.-L.; Guo, G.-C.; Cai, L. Z.; Zhang, Z.-J.; Huang, J.-S. *Inorg. Chem.* **2005**, *44*, 184.

exploring the role of template cations in constructing the inorganic framework structures of chalcogenoarsenates. During our pursuit, we reported three selenoarsenates, $[\text{Mn}(\text{dien})_2]_3(\text{As}_3\text{Se}_6)_2$, $[\text{Fe}(\text{en})_3](\text{As}_2\text{Se}_6)$, and $[\text{Mn}(\text{en})_3](\text{As}_2\text{Se}_6)$,¹⁰ and two unprecedented thioarsenates, $[\text{Mn}(\text{dien})_2]_n$ - $[\text{Mn}(\text{dien})\text{AsS}_4]_{2n} \cdot 4n\text{H}_2\text{O}$ and $[\text{Mn}(\text{en})_3]_2[\text{Mn}(\text{en})_2\text{AsS}_4](\text{As}_3\text{S}_6)$, which are the first two examples of chalcogenoarsenate(V) incorporated with tm amine complexes.^{7d} By using the tetradentate amine ligand (triethylenetetramine) as a structure-directing agent, we have recently obtained one compound, $\text{Mn}_2(\text{C}_6\text{H}_{18}\text{N}_4)_2\text{As}_2\text{S}_5 \cdot 0.25\text{H}_2\text{O}$, in which a tm amine complex is incorporated into chalcogenarsenate(III) framework.¹¹ Inspired by these, we are now using the rigid chelating ligand 2,2'-bipy as a structure-directing agent for the purpose of obtaining chalcogenoarsenates incorporated with tm amine complexes, which resulted in two novel compounds, $[\text{Mn}_3(2,2'\text{-bipy})_3(\text{As}^{\text{V}}\text{S}_4)_2]_n \cdot n\text{H}_2\text{O}$ (**1**) and $\text{Mn}_2(2,2'\text{-bipy})\text{As}_2^{\text{III}}\text{S}_5$ (**2**), with the main-group chalcogenide framework incorporated with a $[\text{tm}(2,2'\text{-bipy})_m]^{n+}$ complex.

Experimental Section

Materials and Instrumentation. All reagents were purchased commercially and used without further purification. Elemental analyses (C, H, N, and O) were performed on an Elementar Vario EL III microanalyzer. A NETZSCH STA 449C thermogravimetric analyzer was used to obtain TGA and DSC curves in N_2 with an increasing temperature rate of $10\text{ }^\circ\text{C}/\text{min}^{-1}$ in the temperature range $30\text{--}600\text{ }^\circ\text{C}$. An empty Al_2O_3 crucible was used as reference. The FT-IR spectra were obtained on a Perkin-Elmer spectrophotometer using KBr disks in the range $4000\text{--}400\text{ cm}^{-1}$. The solid-state fluorescence excitation and emission spectra were performed on a JY FluoroMax-3 spectrophotometer at room temperature with a wavelength increment of 1.0 nm and integration time of 0.1 s. Optical diffuse reflectance spectra were measured at room temperature with a PE Lambda 35 UV-vis spectrophotometer. The instrument was equipped with an integrating sphere and controlled by a personal computer. The samples were ground into fine powder and pressed onto a thin glass slide holder. The BaSO_4 plate was used as a standard (100% reflectance). The absorption spectra were calculated from reflectance spectra using the Kubelka-Munk function: $\alpha/S = (1 - R)^2/2R$,¹² where α is the absorption coefficient, S is the scattering coefficient (which is practically

wavelength independent when the particle size is larger than $5\text{ }\mu\text{m}$), and R is the reflectance. Magnetic susceptibilities were measured by using a PPMS 9T Quantum Design SQUID magnetometer. All data were corrected for diamagnetism estimated from Pascal's constants.

Preparation of $[\text{Mn}_3(2,2'\text{-bipy})_3(\text{As}^{\text{V}}\text{S}_4)_2]_n \cdot n\text{H}_2\text{O}$ (1**).** A mixture of MnCO_3 (115 mg, 1 mmol), arsenic (75 mg, 1 mmol), sulfur (224 mg, 7 mmol), and 2,2'-bipy (78 mg, 0.5 mmol) in 5 mL of distilled water was sealed in a 25 mL poly(tetrafluoroethylene)-lined stainless steel container under autogenous pressure and then heated at $180\text{ }^\circ\text{C}$ for 7 days and cooled to room temperature for more than 3 h. Orange crystals of **1** were filtered, washed with dry diethyl ether, and collected in ca. 65% yield (on the basis of manganese). Anal. Calcd for **1**, $\text{C}_{30}\text{H}_{26}\text{As}_2\text{Mn}_3\text{N}_6\text{O}_8$: C, 34.07; H, 2.48; N, 7.95. Found: C, 34.88; H, 2.77; N, 8.04. FT-IR (KBr, cm^{-1}): 1600–1400 (C=C and C=N).

Preparation of $\text{Mn}_2(2,2'\text{-bipy})\text{As}_2^{\text{III}}\text{S}_5$ (2**).** The complex was prepared in a manner analogous to that of **1**, except a solvent mixture of 0.1 mL of dien and 5 mL of water was used instead. Red crystals of **2** were filtered, washed with dry diethyl ether, and collected in ca. 55% yield (on the basis of manganese). Anal. Calcd for **2**, $\text{C}_{10}\text{H}_8\text{As}_2\text{Mn}_2\text{N}_2\text{S}_5$: C, 20.85; H, 1.40; N, 4.86. Found: C, 20.12; H, 1.15; N, 4.98. FT-IR (KBr, cm^{-1}): 1600–1400 (C=C and C=N).

Single-Crystal Structure Determinations. Single crystals of **1** and **2** were mounted on a Rigaku Mercury CCD diffractometer equipped with graphite-monochromated Mo $\text{K}\alpha$ radiation by using a ω scan technique at 293 K; CrystalClear¹³ software was used for data reduction. The structures were solved by the direct method using the Siemens SHELXTL, version 5, package of crystallographic software.¹⁴ The difference Fourier maps created on the basis of these atomic positions yield the other non-hydrogen atoms. The structure was refined using a full-matrix least-squares refinement on F^2 . All non-hydrogen atoms were refined anisotropically. Hydrogen atoms of 2,2'-bipy were added according to theoretical models. Hydrogen atoms of water molecules in **1** were not added. Crystallographic data and structural refinements for **1** and **2** are summarized in Table 1. More details on the crystallographic studies as well as atom displacement parameters are given in the Supporting Information.

Results and Discussion

Synthetic Consideration. Two novel complexes with very different structures were obtained in similar reaction procedures, except that 0.1 mL of dien was added in the formation of **2**. The dien in the formation of **2** acts as an organic base to justify the pH value of the aqueous solution, which can be replaced by en. Detailed experiments suggest that the yield of **2** is lower (about 35%) when dien is substituted by en in the reaction. Compound **2** cannot be obtained if $\text{NH}_3 \cdot \text{H}_2\text{O}$ is used instead, if the amount of dien is more than 0.15 mL, or if manganese metal is used as a starting material. The temperature does not play a decisive role in the formation of the two compounds, although it is directly related to the yields of the products. The two compounds could also be obtained in a lower yield by using a similar procedure in

- (8) (a) Schaefer, M.; Näther, C.; Lehnert, N.; Bensch, W. *Inorg. Chem.* **2004**, *43*, 2914. (b) Schaefer, M.; Engelke, L.; Bensch, W. *Z. Anorg. Allg. Chem.* **2003**, *629*, 1912. (c) Schaefer, M.; Näther, C.; Bensch, W. *Solid State Sci.* **2003**, *5*, 1135. (d) Stähler, R.; Bensch, W. *Eur. J. Inorg. Chem.* **2001**, 3073. (e) Stähler, R.; Bensch, W. *J. Chem. Soc., Dalton Trans.* **2001**, 2518. (f) Stähler, R.; Bensch, W. *Acta Crystallogr., Sect. C* **2001**, *57*, 26. (g) Vaquero, P.; Chippindale, A. M.; Powell, A. V. *Polyhedron* **2003**, *22*, 2839.
- (9) (a) Chou, J.-H.; Hanko, J. A.; Kanatzidis, M. G. *Inorg. Chem.* **1997**, *36*, 4. (b) Kanatzidis, M. G.; Chou, J.-H. *J. Solid State Chem.* **1996**, *127*, 186. (c) Iyer, R. G.; Kanatzidis, M. G. *Inorg. Chem.* **2004**, *43*, 3656. (d) Wood, P. T.; Schimek, G. L.; Kolis, J. W. *Chem. Mater.* **1996**, *8*, 721. (e) Jerome, J. E.; Wood, P. T.; Pennington, W. T.; Kolis, J. W. *Inorg. Chem.* **1994**, *33*, 1733. (f) O'Neal, S. C.; Pennington, W. T.; Kolis, J. W.; *J. Am. Chem. Soc.* **1991**, *113*, 710. (g) Cordier, G.; Schwidetzky, C.; Schäfer, H. *Z. Naturforsch., B: Chem. Sci.* **1985**, *40*, 1. (h) Wachhold, M.; Sheldrick, W. S. *Z. Naturforsch., B: Chem. Sci.* **1996**, *51*, 32. (i) An, Y.; Li, X.; Liu, X.; Ji, M.; Jia, C. *Inorg. Chem. Commun.* **2003**, *6*, 1137.
- (10) Fu, M.-L.; Guo, G.-C.; Liu, X.; Liu, B.; Cai, L.-Z.; Huang, J.-S. *Inorg. Chem. Commun.* **2005**, *8*, 18.
- (11) Fu, M.-L.; Guo, G.-C.; Liu, X.; Liu, B.; Wang, M.-S.; Huang, J.-S. Unpublished work.

- (12) Wendlandt, W. M.; Hecht, H. G. *Reflectance Spectroscopy*; Interscience: New York, 1966.
- (13) CrystalClear, version 1.35; Rigaku Corp.: Osaka, Japan, 2002.
- (14) Siemens, *SHELXTL Version 5 Reference Manual*; Siemens Energy & Automation Inc.: Madison, WI, 1994.

Table 1. Crystal and Structure Refinement Data for **1** and **2**

	[Mn ₃ (2,2'-bipy) ₃ - (As ^V S ₄) ₂] _n ·nH ₂ O (1)	Mn ₂ (2,2'-bipy)- As ₂ ^{III} S ₅ (2)
formula	C ₃₀ H ₂₆ As ₂ Mn ₃ N ₆ OS ₈	C ₁₀ H ₈ As ₂ Mn ₂ N ₂ S ₅
<i>M_r</i>	1057.71	576.20
cryst size (mm ³)	0.32 × 0.31 × 0.10	0.22 × 0.20 × 0.17
cryst system	orthorhombic	monoclinic
space group	Pbcn	P2 ₁ /c
<i>a</i> (Å)	15.8628(18)	11.198(2)
<i>b</i> (Å)	11.9594(8)	12.228(2)
<i>c</i> (Å)	21.3058(15)	12.3655(19)
β (deg)		105.710(2)
<i>V</i> (Å ³)	4041.9(6)	1629.9(5)
<i>D</i> _{calcd} (Mg m ⁻³)	1.738	2.348
<i>Z</i>	4	4
<i>F</i> (000)	2100	1112
μ (Mo Kα) (mm ⁻¹)	2.995	6.209
no. of reflns collected/unique	25 211/3565	10 246/2870
(<i>R</i> _{int})	(0.0400)	(0.0548)
data/params	3401/231	1914/190
<i>R</i> ^a	0.0497	0.0427
<i>R</i> _w ^b	0.1290	0.0766
GOF	1.044	1.008
Δρ _{max} and Δρ _{min} (e Å ⁻³)	0.904 and -0.449	1.174 and -0.681

$$^a R_1 = \sum(|F_o| - |F_c|) / \sum|F_o|, \quad ^b wR_2 = [\sum w(F_o^2 - F_c^2)^2 / \sum w(F_o^2)^2]^{1/2}.$$

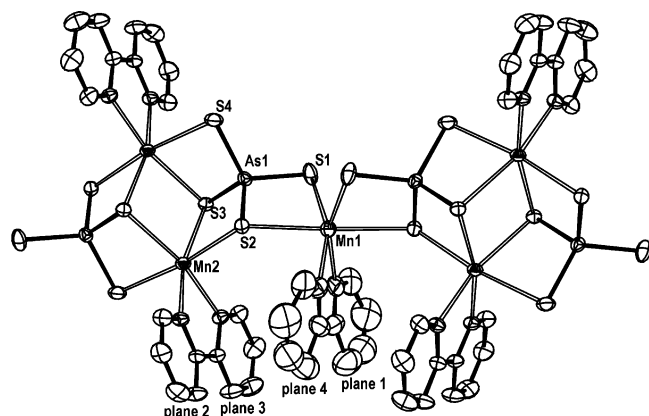


Figure 1. ORTEP view of a [Mn₃(2,2'-bipy)₃(AsS₄)₂]_n neutral chain in **1** with 30% probability level thermal ellipsoids. Hydrogen atoms are omitted for clarity. The distances between ring centroids and dihedral angles between two planes are 3.786(1) Å and 3.9(3)° between planes 1 and 2 and 3.992-(1) Å and 25.7(3)° between planes 3 and 4, where plane 1 contains N11, C11, C12, C13, C14, and C15; plane 2 contains N1, C1, C2, C3, C4, and C5; plane 3 contains N2, C6, C7, C8, C9, and C10; and plane 4 contains N11A, C12A, C13A, C14A, and C15A (A: -x, y, 0.5 - z).

the 150–180 °C range. The remainders of both reactions are found to include MnS, S₈, and some unknown black residues; moreover, sulfated hydrogen must be occurring with the formation of **2** because of the rotten-egg odor.

Crystal Structure Descriptions of 1 and 2. X-ray crystallography reveals that compound **1** consists of one-dimensional [Mn₃(2,2'-bipy)₃(As^VS₄)₂]_n neutral wavelike chains and lattice water molecules. The chain is composed of [Mn(2,2'-bipy)]²⁺ fragments being bridged by [As^VS₄] groups, in which each of two crystallographically independent Mn²⁺ centers is chelated by one 2,2'-bipy ligand and coordinated by four S atoms from two [As^VS₄] groups to form a distorted octahedron with a cis configuration (Figure 1). Two Mn₂ octahedra edge-share to form a [Mn]₂ dimer with a crystallographic inversion center and a Mn²⁺···Mn²⁺ distance of 3.812(1) Å. The [Mn]₂ dimers alternately corner-share with Mn₁ octahedra in the trans mode with a

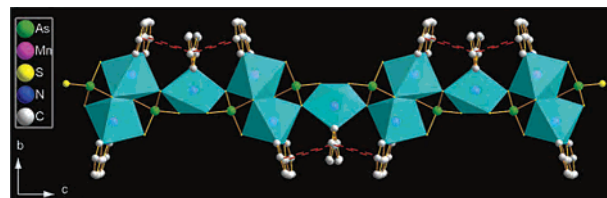


Figure 2. Polyhedral representation of the neutral chain in **1** viewed along the *a* axis; the π···π interactions are shown in red dashed lines. Hydrogen atoms are omitted for clarity.

Mn¹···Mn² distance of 4.784(1) Å to form an undec octahedral chain extending along the *c* direction, whereas the [As^VS₄] tetrahedra multi-edge-share with Mn octahedra (Figure 2). Because of the rigidity of the 2,2'-bipy ligand, the Mn–N bond distances narrowly vary from 2.230(3) to 2.248(2) Å, which are distinguishable from those found in Mn flexible aliphatic amine complexes in which there are great differences among the Mn–N bond distances such as in [Mn(en)_m]²⁺ and [Mn(dien)_m]²⁺.^{7b,7d} The Mn–S bond distances range from 2.5712(9) to 2.6890(7) Å, which are comparable with those reported in the literature.^{7b,7d} The significantly distorted Mn¹ and Mn² octahedra are evident with the axial angles ranging from 157.34(8) to 177.74(4)° and 166.00(6) to 171.18(3)°, respectively, which are consistent with those found for the Mn octahedral geometry coordinated by S and N atoms. Within the chain, there are face-to-face π···π stacking interactions between the two pyridyl rings of 2,2'-bipy chelating to the Mn¹ atom and the adjacent pyridyl rings of 2,2'-bipy chelating to the Mn² atom with centroid–centroid distances of 3.786(1) and 3.992-(1) Å and dihedral angles of 3.9(3) and 25.7(3)°, respectively.

Compound **2** can be regarded as being constructed from basic building units, fused four-cubane [Mn₆(2,2'-bipy)₄-As₆^{III}S₁₄]²⁺, interlinking each other through face-sharing to form a two-dimensional network along the [011] and [01̄1] directions, as shown in Figure 3a. The Mn¹ atom is coordinated by six sulfur atoms from three [As₂^{III}S₅]⁴⁻ groups, with the Mn–S bond distances spreading from 2.567-(1) to 2.728(1) Å, whereas the Mn² atom is chelated by one 2,2'-bipy ligand and coordinated by four sulfur atoms from two [As₂^{III}S₅]⁴⁻ groups, with Mn–N bond distances of 2.225-(3) and 2.242(2) Å; the Mn–S bond distances are in the range 2.543(1)–3.010(1) Å. The significantly distorted MnS₄N₂ octahedra are evident, with axial angles ranging from 160.08-(6) to 175.67(7)°, which are also caused by the steric constraints of ligands and the great difference between Mn–S and Mn–N bond distances. In contrast, those of MnS₆ octahedra are in the narrow range from 173.32(3) to 175.31-(3)°. The geometric features of Mn octahedra are similar to those in **1** and the literature.^{7b,7d} One MnS₆, one MnS₄N₂ octahedra, and two AsS₃ pyramids are connected to form a cubane-like [Mn₂As₂S₄] structure, which is edge-shared through the As¹–S² bonds and corner-shared through the Mn¹ atoms to form a fused four-cubane with a crystallographic inversion center; the Mn···Mn distances are 3.615-(2), 3.643(1), and 3.874(2) Å. (Figure 3b). The fused four-cubane interlink through sharing the Mn²–As²–S⁴–S⁵ face to form a slab extending along the [011] and [01̄1] directions. The slabs are parallelly stacked, resulting in the formation

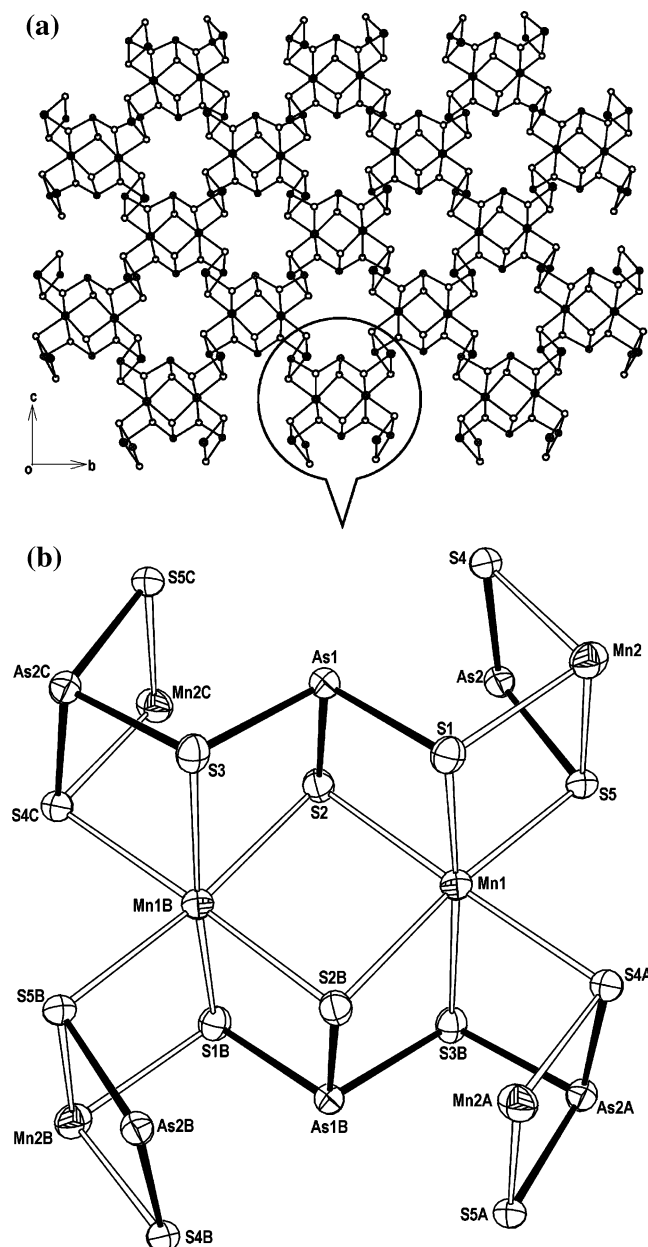


Figure 3. (a) Arrangement of the layers in $\text{Mn}_2(2,2'\text{-bipy})\text{As}_2\text{S}_5$ **2** viewed along the a direction. (b) ORTEP view of the basic building unit, $[\text{Mn}_6(2,2'\text{-bipy})_4\text{As}_6^{\text{III}}\text{S}_{14}]^{2+}$, in **2** as circled in the top diagram; symmetry codes are A ($x, 1/2 - y, -1/2 + z$); B ($1 - x, -y, -z$); C ($1 - x, -1/2 + y, 1/2 - z$). 2,2'-bipy molecules are omitted for clarity.

of channels along the a axis, with the 2,2'-bipy molecules spreading to the pores (Figure 4). An interesting feature of **2** is that there exists a remarkably long $\text{Mn}2\text{-S}2$ bond distance of 3.010(1) and a N-Mn-N bite bond angle of $73.3(1)^\circ$, which is also found in $\text{Mn}_2\text{LSb}_2\text{S}_5$ (L = two monodentate amine such as methyl-, ethyl- or propylamine, or a bidentate one like diaminopropane or ethylenediamine).^{7a,15} It is worthy to note that compound **2** can be expected to be the first example of a new series of compounds formulated as $\text{Mn}_2\text{LAS}_2\text{S}_5$.

Bond-valence sum calculations¹⁶ ($\text{As}1 = 5.278$ for **1** and $\text{As}1 = 2.860$, $\text{As}2 = 2.938$ for **2**) and the average As-S

(15) Schur, M. Ph.D. thesis, edition Wissenschaft, Reihe Chemie 2000; tectum Verlag: Marburg, Germany, 2000; p 301.

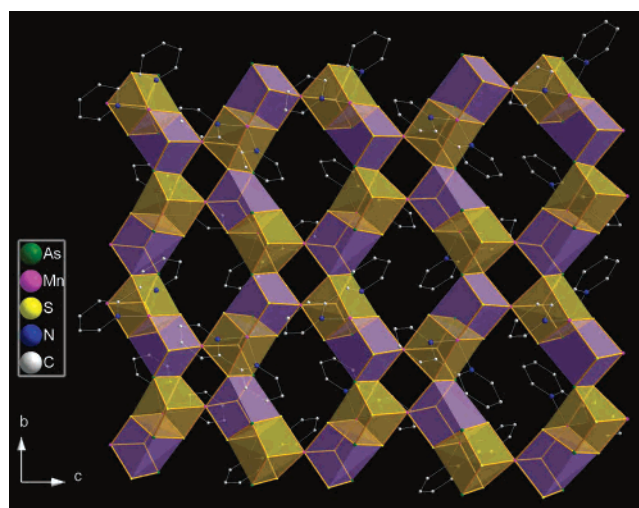


Figure 4. Pack diagram of compound **2** viewed along the a direction showing the channels. The fused four-cubane with a crystallographic inversion center interlinks by sharing the $\text{Mn}2\text{-As}2\text{-S}4\text{-S}5$ face to form a slab extending along the $[011]$ and $[0\bar{1}1]$ directions. Hydrogen atoms are omitted for clarity.

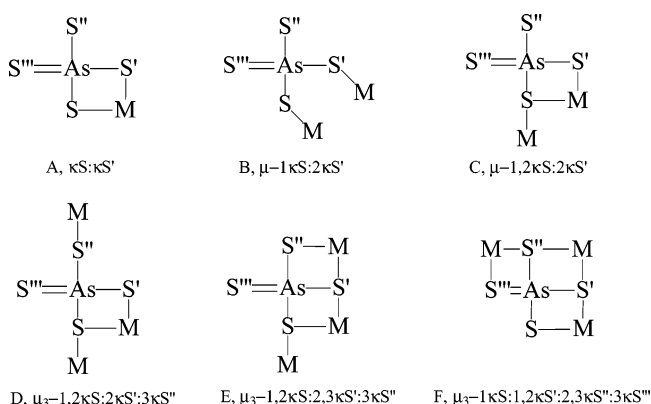


Figure 5. Coordination modes of the $[\text{As}^{\text{V}}\text{S}_4]^{3-}$ anion found in the literature and **1**. F is the novel coordination mode found in **1** for the first time.

bond lengths indicate the oxidation state of As atoms in **1** and **2** should be +5 and +3, respectively. Though tetrahedral $[\text{As}^{\text{V}}\text{S}_4]^{3-}$ and condensed oligomeric $[\text{As}_2^{\text{III}}\text{S}_5]^{4-}$ are the most-dominant anions in metal chalcogenates, the examples of them as ligands coordinated to transition metal complexes are very limited.^{7d,11} The geometric features of tetrahedral $[\text{As}^{\text{V}}\text{S}_4]^{3-}$ in **1** and pyramidal $[\text{As}^{\text{III}}\text{S}_3]^{3-}$ in **2** are similar to those found in the literature.^{7b,7d,9a,17} Despite the $[\text{As}^{\text{V}}\text{S}_4]^{3-}$ anion exhibiting various coordination modes in the literature, in **1**, it acts as a novel $\mu_3\text{-}1\kappa\text{S}:1,2\kappa\text{S}':2,3\kappa\text{S}'':3\kappa\text{S}'''$ coordination mode, which is the first example of all four S atoms of the $[\text{As}^{\text{V}}\text{S}_4]^{3-}$ anion coordinating with metal (Figure 5). Although a variety of compounds of chalcogenoarsenate(III)/chalcogenoantimonate(III) incorporated with tm complexes are known, those with chalcogenoarsenate(V)/chalcogenoantimonate(V) are limited, the known examples being chalcogenoarsenate(V) compounds $[\text{Mn}(\text{dien})_2]_n$ [Mn -

(16) (a) Brese, N. E.; O'Keeffe, M. *Acta Crystallogr., Sect. B* **1991**, *47*, 192. (b) Brown, I. D.; Altermatt, D. *Acta Crystallogr., Sect. B* **1985**, *41*, 244.

(17) Auernhammer, M.; Effenberger, H.; Irran, E.; Pertlik, F.; Rosenstingl, J. *J. Solid State Chem.* **1993**, *106*, 421.

(dien)AsS₄]_{2n}·4nH₂O and [Mn(en)₃]₂[Mn(en)₂AsS₄](As₃S₆)^{7d} and chalcogenoantimonate(V) compounds [Mn(C₆H₁₈N₄)-(C₆H₁₉N₄)]SbS₄,^{8b} [Mn(C₆H₁₄N₂)₃]₂[Mn(C₆H₁₄N₂)₂(SbS₄)₂]·6H₂O,^{8b} Ni[N(CH₂CH₂NH₂)₃](SbS₄),^{8f} and [Mn(en)₃]₂[Mn₄(en)₉(SbSe₄)₄]·2H₂O,^{7c} in which the coordination modes of the tetrachalcogenoantimonate(V) anion are different than that in **1**.

TGA Study. Thermogravimetric analysis of **1** reveals two distinct steps with weight changes of about 56.06 and 20.70% before 500 °C, accompanied by two obvious endothermic peaks (see the Supporting Information, Figure S2), that correspond to the removal of the water molecules and 2,2'-bipy ligands (calcd 46.00%), the emission of H₂S (calcd 9.67%), and the removal of As₂S₂ (calcd 20.23%). As in **2**, it shows a three-step weight loss (10.94, 36.19, and 23.78%) before 500 °C (see the Supporting Information, Figure S3). The observed total weight losses (70.91%) are comparable with the removal of 2,2'-bipy ligands (calcd 27.10%), the emission of H₂S (calcd 5.91%), and the removal of As₂S₂ (calcd 37.13%). Both residues of the compounds are calculated to be MnS (For **1**, exp. 23.24%, calcd 24.1%; For **2**, exp. 29.09%, calcd 29.86%).

Luminescence Properties and Optical Spectroscopy. The two compounds are photoluminescence materials with an emission maximum occurring at about 440 nm ($\lambda_{ex} = 365$ nm; see the Supporting Information, Figure S4), which is similar to those found for similar compounds [Mn(dien)₂]_n[Mn(dien)AsS₄]_{2n}·4nH₂O and [Mn(en)₃]₂[Mn(en)₂AsS₄](As₃S₆)^{7d} and the analogues of main-group chalcogenide.³ However, the mechanism of this phenomenon may be complicated and has not been elucidated so far.³ We consider that the emissions of **1** and **2** are likely related to the emission of an organic component. Furthermore, the reflectance data suggest that the two compounds are semiconductors ($E_g = 2.18$ eV (**1**), 1.83 eV (**2**); see the Supporting Information, Figure S5), which is consistent with the color of their crystals. The electronic transition is likely a result of charge transfer from the S²⁻-dominated valence band to the Mn²⁺-dominated conduction band.¹⁸

Magnetic Properties. Magnetic measurements of hand-picked single crystals of **1** and **2** were performed; the crystals' purities were confirmed by PXRD (see the Supporting Information, Figure S6), in a field of 1 T and a 2–300 K temperature range. Temperature dependencies of the molar magnetic susceptibility (χ_M) of **1** (Mn₃) and **2** (Mn₂) and the effective magnetic moment (μ_{eff}) per Mn²⁺ are presented in Figure 6. On lowering temperature, molar magnetic susceptibilities (χ_M) increase until they reach a maximum at 0.104 and 0.0526 emu⁻¹ mol and then decrease gradually, which shows antiferromagnetic ordered states with Néel temperatures of 19 and 24 K for **1** and **2**, respectively. The plots of the reciprocal susceptibilities (χ_M^{-1}) show the data to significantly deviate from the Curie–Weiss law ($1/\chi_M = (T-\theta)/C$) below 100 K (see the Supporting Information, Figure S7). The linear behaviors of the inverse

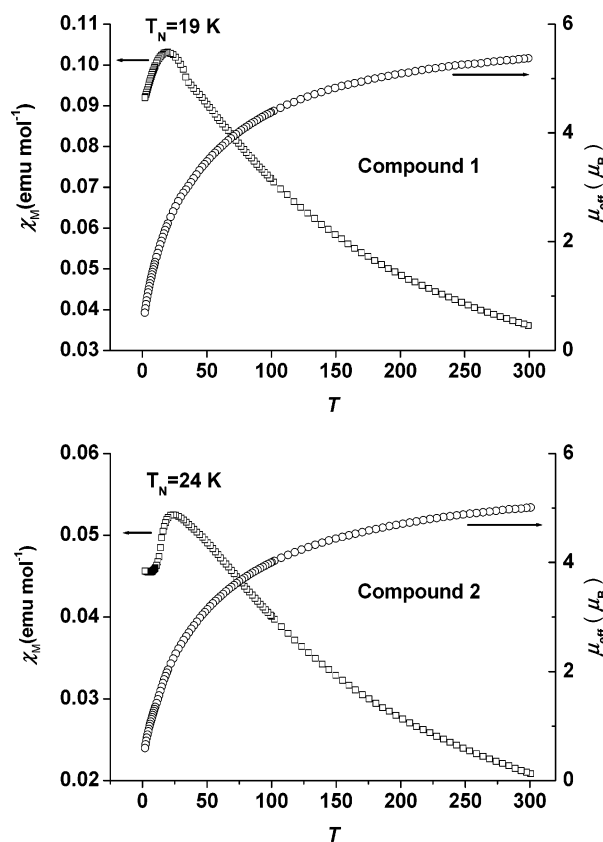


Figure 6. χ_M of **1** (Mn₃) and **2** (Mn₂) vs T and μ_{eff} (per Mn²⁺) vs T plots for **1** and **2**.

susceptibilities above 100 K yield $C = 14.38(4)$ emu mol⁻¹ K, $\theta = -97.4(8)$ for **1**, and $C = 8.72(2)$ emu mol⁻¹ K, $\theta = -115.8(6)$ K for **2**. These lead to effective magnetic moments per Mn ion of 6.19 and 5.91 μ_B for **1** and **2**, respectively, which are comparable to the expected spin-only value of 5.92. The rather negative values of the Weiss constants indicate the presence of rather strong antiferromagnetic coupling between Mn ions in both compounds, which can also be shown from the unsaturated behaviors of the $M(H)$ of both compounds at 2 K under 9 T (see the Supporting Information, Figure S8). The S²⁻ ligand may be responsible for the strong AF interaction between Mn ions, which has been also reported in the chalcogenides of Ba₂MnS₃.¹⁹ To the best of our knowledge, the metal chalcogenides incorporated with an organic ligand and showing an antiferromagnetic order have been found for the first time. We have been unsuccessful in finding a model to fit the magnetic data for both compounds.

Conclusion

In summary, two interesting tm chalcogenoarsenate compounds, [Mn₃(2,2'-bipy)₃(As^VS₄)₂]_n·nH₂O (**1**) and Mn₂(2,2'-bipy)As₂^{III}S₅ (**2**), in which the main-group chalcogenide framework is incorporated with a [tm(2,2'-bipy)_m]ⁿ⁺ complex, have been synthesized and structurally characterized. The two compounds exhibit semiconducting properties and strong

(18) (a) Herron, N.; Suna, A.; Wang, Y. *J. Chem. Soc., Dalton Trans.* **1992**, 2329. (b) Wang, Y.; Harmer, M.; Herron, N. *Isr. J. Chem.* **1993**, 33, 31.

(19) (a) Grey, I. E.; Steinfink, H. *Inorg. Chem.* **1971**, 10, 691. (b) Greaney, M. A.; Ramanujachary, K. V.; Teweldemedhin, Z.; Greenblatt, M. *J. Solid State Chem.* **1993**, 107, 554.

blue photoluminescence. Magnetic measurements show that both compounds have AF ordered states with Néel temperatures of 19 and 24 K for **1** and **2**, respectively.

Acknowledgment. We gratefully acknowledge the financial support of the NSF of China (20131020), the NSF for Distinguished Young Scientists of China (20425104) and the NSF of the Fujian Province (Z0513019).

Supporting Information Available: X-ray crystallographic files in CIF format for the structure determination of **1** and **2**, TGA curves, IR spectra, optical absorption spectra, solid emission spectra, field dependent magnetizations, and PXRD patterns of **1** and **2**. This material is available free of charge via the Internet at <http://pubs.acs.org>.

IC0600228